# Conformational Analysis of the Cyclic Pentadepsipeptide Cyclo(Tro-Aib-Aib-Aib-Aib) in the Solid State and in Solution

by **Kristian N. Koch**[1]), **Gudrun Hopp**, **Anthony Linden**, **Kerstin Moehle**, and **Heinz Heimgartner***

Organisch-chemisches Institut der Universität Zürich, Winterthurerstrasse 190, CH-8057 Zürich

The cyclic 16-membered pentadepsipeptide cyclo(Tro-Aib-Aib-Aib-Aib) (**1**) was crystallized from MeOH/AcOEt/$CH_2Cl_2$, and its structure was established by X-ray crystallography (*Fig. 1*). There are two symmetry-independent molecules with different conformations in the asymmetric unit. Two intramolecular H-bonds stabilize two $\beta$-turns in each molecule. On the other hand, two of the four Aib residues are forced to assume a nonfavorable nonhelical conformation in each of the symmetry-independent molecules (*Table 1*). The conformational study in $CDCl_3$ solution by NMR spectroscopy and molecular dynamics (MD) simulations indicate that the averaged structure (*Fig. 3*) is almost the same as in the solid state.

**1. Introduction.** – Cyclization of a peptide chain has been used extensively as a method for introducing conformational constraints in the peptide backbone. When $\alpha,\alpha$-disubstituted $\alpha$-amino acids such as aminoisobutyric acid (Aib, 2,2-dimethylglycine) are incorporated into the cyclic peptide chain, the conformational flexibility of the peptide backbone is limited further.

Replacement of the H–C($\alpha$) atom by a Me group, as in the Aib residue, leads to severe restrictions of the conformational freedom [1–5]. Calculations of the allowed torsion angles $\phi$ and $\psi$ for the Aib residue have shown that they are found in two very confined regions near $\phi = \pm 57°$ and $\psi = \pm 47°$ in the *Ramachandran* plot [3]. These two regions correspond to the right-handed and the left-handed $\alpha$-helix/$3_{10}$-helix, respectively. A large number of peptides containing Aib residues have had their structures established by X-ray crystallography [6–12]. It could be concluded from these structures that the Aib residue is a strong promoter of secondary structures, such as $\beta$-turns and $\alpha$- and $3_{10}$-helices [1–5].

The cyclic tetrapeptide *chlamydocin* [6] and the cyclic pentapeptides cyclo(Phe-Phe-Aib-Leu-Pro) [7], cyclo(Gly-(*R*)-Phe(2Me)-Aib-Aib-Gly) [11], cyclo(Gly-Aib-(*R*)-Phe(2Me)-Aib-Gly) [12], and cyclo(Gly-(*R*)-Phe(2Me)-Pro-Aib-Phe) [12] each contain one Aib residue with torsion angles in the nonhelical conformational space (*i.e.*, well away from the $\phi$ and $\psi$ angles mentioned above). Furthermore, Aib takes part in the formation of a $\gamma$-turn in position $i+1$ in some of these cyclic peptides [6][7][12], which is rather unusual for the Aib residue. These data show that Aib can be forced to assume a nonhelical conformation when this facilitates the formation of the cyclic structure and leads to the release of intramolecular strain.

Based on these precedents, it was of interest to analyze the conformation of a cyclic pentadepsipeptide containing more than one Aib residue by X-ray crystallography,

[1]) Part of the Ph.D. thesis of *K.N.K.*, Universität Zürich, 2000.

and, in solution, by NMR spectroscopy and molecular-dynamics simulations. The objective was to study the conformational preferences of the Aib residues, to determine which positions in the $\phi$, $\psi$ space they would occupy, and to compare the conformations of the cyclic depsipeptide in the solid state and in solution.

**2. Results and Discussion.** – The racemic cyclic pentadepsipeptide cyclo(Tro$^1$-Aib$^2$-Aib$^3$-Aib$^4$-Aib$^5$) (**1**) was crystallized from MeOH/AcOEt/$CH_2Cl_2$, and its structure was established by X-ray crystallography (*Fig. 1*). The synthesis of **1** has been described previously [13].

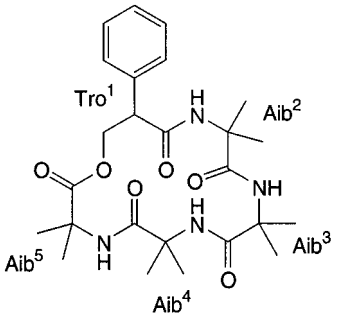


**1**

2.1. *Solid-State Conformation.* There are two symmetry-independent molecules, A and B, in the asymmetric unit, and their conformations differ, both in the orientation of the Ph ring and in slightly different puckering of the macrocyclic ring. As a result of these different conformations, each of the independent molecules forms a slightly different pattern of H-bonds. The relevant torsion angles of the two molecules are given in *Table 1*; the intra- and intermolecular H-bond parameters are listed in *Table 2*.

In molecule A, the torsion angles ($\phi$, $\psi$) for Aib$^3$ and Aib$^5$ are in good agreement with the expected values in the helical region of the *Ramachandran* plot, but the Aib$^2$ and Aib$^4$ residues have torsion angles that lie in the nonhelical region. In molecule B, the torsion angles for Aib$^2$ and Aib$^3$ were found to be similar to those of molecule A, but the torsion angles for Aib$^4$ and Aib$^5$ deviate significantly from the values found for molecule A: Aib$^4$ has torsion angles in the helical region, whereas the torsion angles for Aib$^5$ lie in the nonhelical region.

All the amide bonds have the s-*trans*-configuration ($|\omega| = 154.7 - 177.6°$) and the ester bonds also show the s-*trans*-configuration, but some of these amide and ester bonds deviate significantly from planarity (*cf.* [15]). Each of the independent molecules A and B adopts two consecutive $\beta$-turns stabilized by the intramolecular H-bonds N(3)–H$\cdots$O(10) and N(6)–H$\cdots$O(13) for molecule A and N(33)–H$\cdots$O(40) and N(36)–H$\cdots$O(43) for molecule B (*Table 2*), although the second interaction in molecule B is extremely weak (*cf.* [16]). The combination of the torsion angles for the two residues Aib$^3$ and Aib$^4$ ($\phi_3$, $\phi_4$, and $\psi_3$, $\psi_4$) are in good agreement with the values of a distorted $\beta$-turn conformation of type I (I′) for molecule A and close to the ideal values for a $\beta$-turn conformation of type III (III′) for molecule B. Molecule A forms two intermolecular H-bonds from N(9)–H and N(12)–H to O(34′) and O(37″),

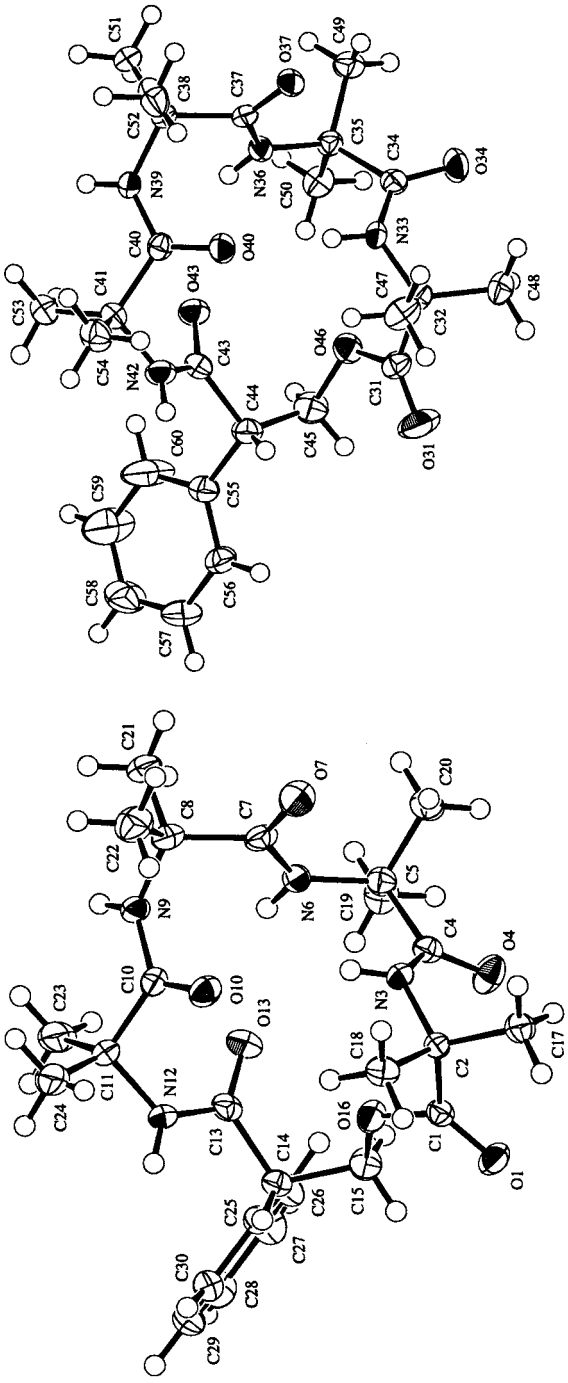


Fig. 1. *ORTEP Plot* [14] *of the molecular structures of molecule A and B of* **1** (arbitrary numbering of the atoms; 50% probability ellipsoids)

Table 1. *Selected Intra-annular Torsion Angles of the Two Crystallographically Independent Molecules A and B of* **1**

| Residue | Angle [°] | Molecule A | Molecule B |
|---|---|---|---|
| Tro[1] | $\phi_1$ | 156.6(2) | 83.7(3) |
| | $\chi_1$[a]) | 46.2(3) | 52.4(3) |
| | $\psi_1$ | −133.6(2) | −152.5(2) |
| | $\omega_1$ | −176.9(2) | 177.6(1) |
| Aib[2] | $\phi_2$ | −55.4(3) | −52.5(3) |
| | $\psi_2$ | 136.3(2) | 136.2(2) |
| | $\omega_2$ | 170.2(2) | 166.5(2) |
| Aib[3] | $\phi_3$ | 55.5(3) | 51.1(3) |
| | $\psi_3$ | 31.4(3) | 40.8(3) |
| | $\omega_3$ | 169.2(2) | 165.8(2) |
| Aib[4] | $\phi_4$ | 92.1(3) | 71.0(3) |
| | $\psi_4$ | −25.4(3) | 23.1(3) |
| | $\omega_4$ | 174.8(2) | 154.7(2) |
| Aib[5] | $\phi_5$ | −51.9(3) | −99.9(3) |
| | $\psi_5$ | −42.9(3) | 6.4(3) |
| | $\omega_5$[b]) | 167.3(2) | −169.5(2) |

[a]) Torsion angle of the C(2)–C(3) bond of the $\beta$-hydroxy acid Tro. [b]) Torsion angle of the lactone bond.

Table 2. *Selected Inter- and Intramolecular H-Bond Parameters for* **1**

| Molecule | Type[a]) | H···O [Å] | N···O [Å] | N–H···O [°] |
|---|---|---|---|---|
| A | N(9)–H···O(34′) | 2.22(3) | 3.070(3) | 164(2) |
| | N(12)–H···O(37″) | 2.08(2) | 2.957(3) | 174(2) |
| | N(3)–H···O(10) | 2.45(2) | 3.263(2) | 163(2) |
| | N(6)–H···O(13) | 2.48(2) | 3.215(3) | 147(2) |
| B | N(39)–H···O(7‴) | 2.40(2) | 3.144(3) | 149(2) |
| | N(42)–H···O(1) | 2.06(3) | 2.938(3) | 175(3) |
| | N(33)–H···O(40) | 2.33(2) | 3.142(3) | 162(2) |
| | N(36)–H···O(43) | 2.67(2) | 3.367(3) | 143(2) |

[a]) Primed atoms refer to molecules in the following symmetry-related positions: ′: $x, y, 1+z$; ″: $1/2-x, -1/2+y, -1/2-z$; ‴: $-1/2+x, 3/2-y, -1/2+z$.

respectively, of two different neighboring type B molecules (*Table 2*). Molecule B also forms two intermolecular H-bonds from the same amide groups, N(39)–H and N(42)–H, to two different neighboring type-A molecules, but the corresponding acceptor atoms are O(7‴) and O(1), respectively. The intermolecular interactions link the molecules into a three-dimensional network (*Fig. 2*).

Recently, we reported the crystal structure of the cyclic pentadepsipeptide cyclo(Tro[1]-$Ac_5c^2$-$Ac_5c^3$-$Ac_5c^4$-$Ac_5c^5$) (**2**) [13]. The $Ac_5c$ residues belong to the 1-aminocycloalkane-1-carboxylic acids ($Ac_nc$), the family of cyclic $\alpha$,$\alpha$-disubstituted $\alpha$-amino acids. The preferred conformations reported for the $Ac_nc$ residues, apart from the $Ac_3c$ residue, parallel those of the Aib residue [1][17].

In the cyclic depsipeptide **2**, there are four symmetry-independent molecules in the asymmetric unit. The macrocyclic rings in the four independent molecules are very similar without significant conformational differences. The torsion angles ($\phi$, $\psi$) for the $Ac_5c$ residues occupying corresponding positions in each of the four independent

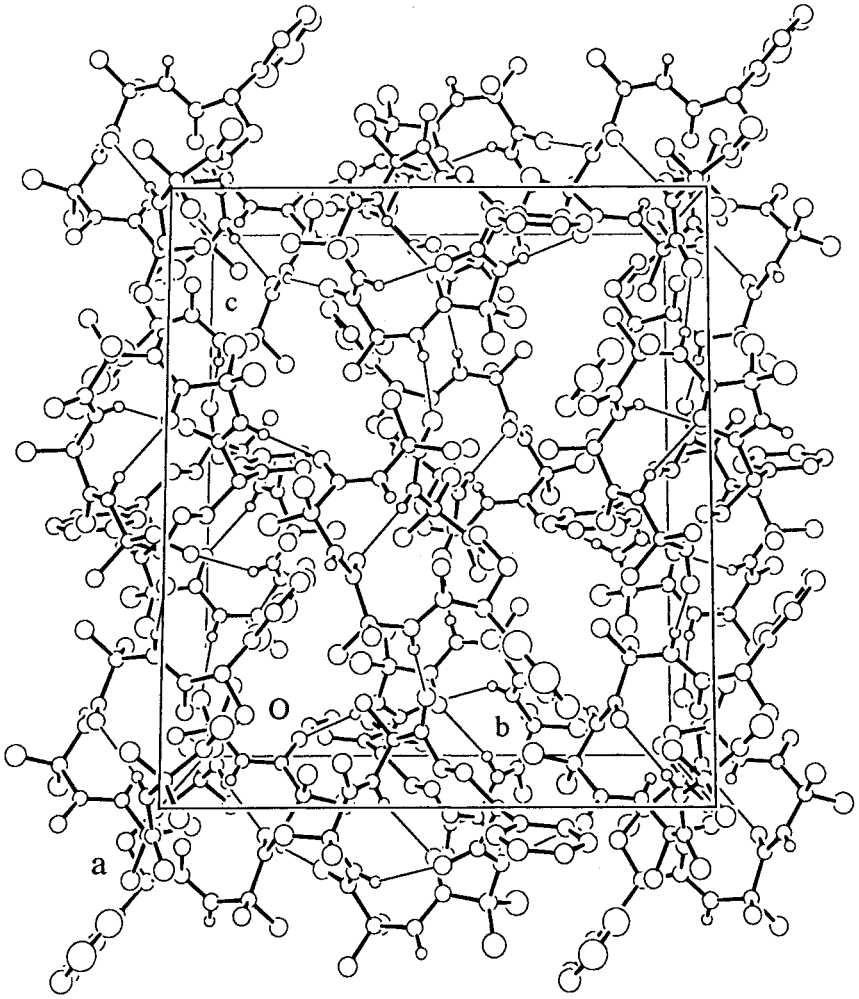


Fig. 2. *Packing diagram of compound* **1**, *showing the H-bonding*

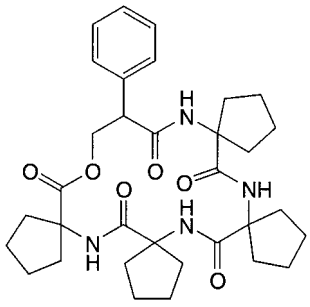


**2**

molecules are comparable. The residues $Ac_5c^3$ and $Ac_5c^5$ have a helical conformation, and those in positions 2 and 4 have a nonhelical conformation in all four independent molecules. A comparison of the torsion angles of the four Aib residues in molecule A of **1** with those of **2** reveals a pronounced similarity. Therefore, it can be concluded that the behaviors of the Aib and $Ac_5c$ residues in the cyclic depsipeptides **1** and **2** are conformationally identical. In both cyclic depsipeptides, two of the $\alpha,\alpha$-disubstituted $\alpha$-amino acids have torsion angles in the nonhelical conformational space, which makes the ring formation possible and results in the release of intramolecular strain.

2.2. *Solution Conformational Analysis.* The conformation of the enantiomerically pure cyclic pentadepsipeptide ((*R*)-Tro$^1$-Aib$^2$-Aib$^3$-Aib$^4$-Aib$^5$) (*R*)-**1**[2]) in $CDCl_3$ solution has been studied by NMR spectroscopy. The measurements have been carried out in the temperature range of 260–300 K. In the $^1$H-NMR spectrum at 275 K, only one set of sharp signals could be observed, but it could not be determined whether this was due to the presence of one major conformer, or due to a high rate of exchange between different conformers. Assignment of all the different $^1$H- and $^{13}$C-NMR signals in (*R*)-**1** was carried out by HSQC and HMBC techniques.

The temperature coefficients of the amide NH resonances are collected in *Table 3*, which shows the NH $\Delta\delta/\Delta T$ values measured in the range of 279–314 K. The value of NH $\Delta\delta/\Delta T$ for Aib$^4$ is zero, which indicates significant shielding from the solvent. The other NH protons have values that indicate that they are more or less freely exposed to the solvent. The relative exchange rates of the amide NH protons were measured by monitoring the disappearance of their resonances upon addition of $CD_3OD$ at 300 K. The NH proton of Aib$^4$ exhibited a half-life of several minutes, whereas the other three NH protons exchanged completely within a few minutes. These two independent experiments indicate that the amide NH of Aib$^4$ participates in an intramolecular H-bond, *e.g.*, the formation of a $\beta$-turn with the C=O group of Tro, which is in agreement with the solid-state structure.

Table 3. *Temperature Coefficients for Amide NH of* (R)-**1** *in the Range of 279–314 K*

| Residue | Aib$^2$ | Aib$^3$ | Aib$^4$ | Aib$^5$ |
|---|---|---|---|---|
| $-\Delta\delta/\Delta T$ [ppb/K] | 4.3 | −1.1 | 0 | 1.7 |

From the NMR ROESY experiment ($T$ = 275 K), a number of structure models of the cyclic depsipeptide (*R*)-**1** were calculated with *DYANA-1.5* [19]. This set of starting structures is rather diffuse with respect to the backbone torsion angles (without indication of the preferred solution structure), because of the missing ROE constraints of the protons at C($\alpha$). Only two significant ROE constraints (sequential distances, $d_{nn}$) could be used to predict the backbone orientation, namely those between NH of Aib$^3$ and NH of Aib$^4$, and between NH of Aib$^4$ and NH of Aib$^5$, but no other ROE constraints between non-neighboring residues were found. No further ROEs were used, because it was not possible to distinguish between the Me side chains in the Aib residue and to add corrections to the ROE distance constraints.

---

[2]) The cyclic pentadepsipeptide (*R*)-**1** was prepared as previously described for racemic **1** [13] starting from (*R*)-tropic acid [18].

Beginning with the starting structure of (*R*)-**1** (minimal DYANA target function), the MD simulations were performed *in vacuo* and in solution. A well-stabilized structure (*Fig. 3*) was found, which displays torsion angles (*Table 4*) that are in good agreement with those found for the two independent molecules A and B in the solid state. This structure includes two Aib-residues ($Aib^3$, $Aib^5$) in the helical conformational region. Additionally, the MD simulations indicate the presence of a strong H-bond (93%) between NH of $Aib^4$ and CO of $Tro^1$ ($d(H\cdots O) = 2.5$ Å, $N-H\cdots O = 129°$). This is in agreement with the experimentally found shielding of the NH of $Aib^4$. The structure of conformer I is consistent with the two observed ROEs.

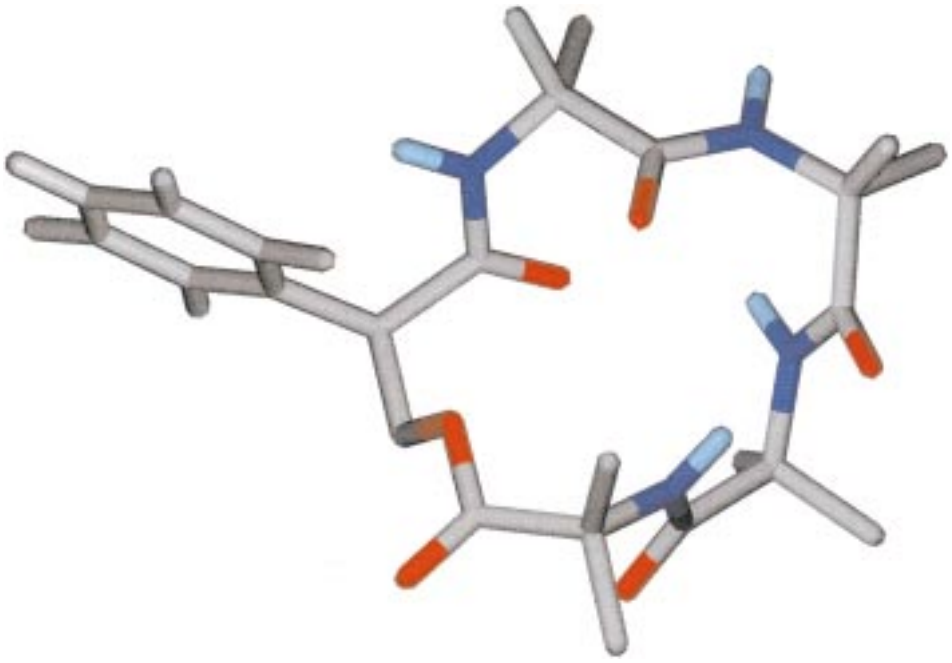

Fig. 3. *Average structure obtained from MD simulations in solution*

It should be mentioned that further conformations could be observed during MD simulations, starting from the variety of NMR model structures without NMR restraints. Due to the restricted flexibility of this molecule containing two methyl side chains at the C($\alpha$)-atoms, it is not possible to overcome more unfavored conformational regions within the simulation time scale. Further simulations were performed starting from the crystal structures A and B. Interestingly, it could be seen that both structures translate in solution into the average conformation described above. As shown in *Fig. 4*, the backbone conformations of the two crystal structures A and B are almost identical with the average solution structure, although some torsion angles for the structure B deviate significantly (*Table 4*).

**3. Conclusions.** – The structure and conformational behavior of the cyclic pentadepsipeptide cyclo($Tro^1$-$Aib^2$-$Aib^3$-$Aib^4$-$Aib^5$) (**1**) have been elucidated by

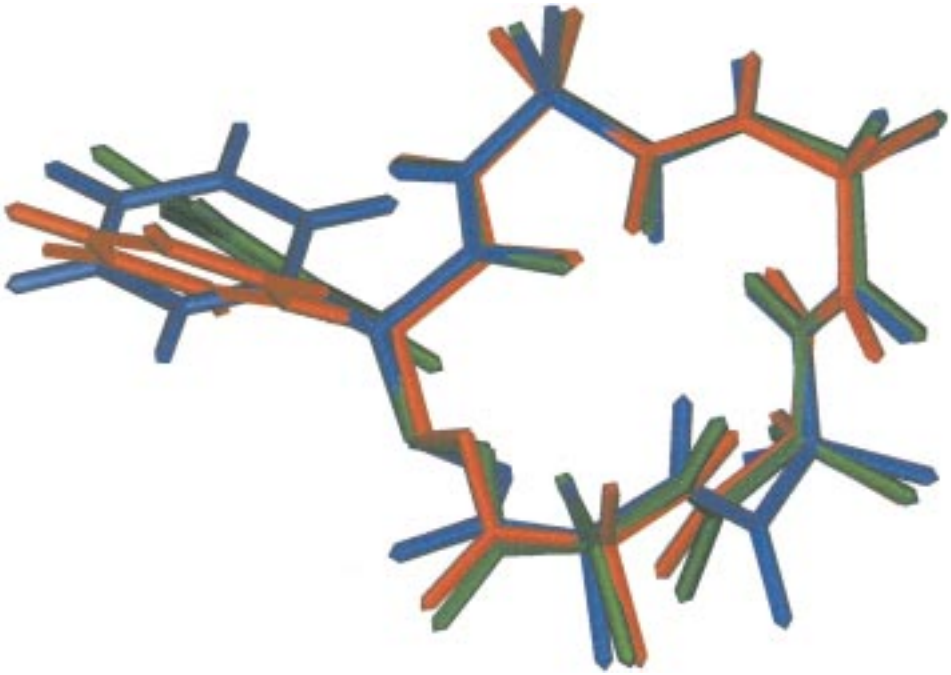

Fig. 4. *Superimposition over the backbone N-, C(α)-, and C-atoms of the average solution structure and the crystal structures A and B* (united atom model; green: crystal A; blue: crystal B; orange: average solution structure)

Table 4. *Averaged Torsion Angles* [°] *for Conformer I of the Pentapeptide* (*R*)-**1** *Obtained from MD Simulations in Solution*

| Residue | $\phi$ | $\psi$ | $\omega$ | $\chi$ |
|---|---|---|---|---|
| Tro[1] | 179.9 ± 10.7 | – 116.7 ± 16.6 | 170.6 ± 7.0 | 54.6 ± 9.2 |
| Aib[2] | – 51.9 ± 9.8 | 130.5 ± 16.2 | – 174.9 ± 6.3 | |
| Aib[3] | 50.9 ± 10.7 | 43.8 ± 31.4 | 178.1 ± 7.2 | |
| Aib[4] | 76.5 ± 11.0 | – 33.9 ± 10.8 | 179.2 ± 7.7 | |
| Aib[5] | – 56.6 ± 10.4 | – 41.5 ± 12.0 | 125.1 ± 14.7[a]) | |

[a]) Torsion angle of the lactone bond.

X-ray crystallography, and, in solution, by NMR spectroscopy and MD simulations. As a result of the cyclic structure, two of the four Aib residues are forced to assume a nonhelical conformation to allow release of intramolecular strain. This observation for the Aib residue is rare, because similar torsion angles ($\varphi$, $\psi$) for Aib have previously been observed only in the solid-state structure of cyclic tetra- and pentapeptides. A comparison of the solid-state conformation of **1** with the previously published structure of the cyclic pentadepsipeptide cyclo(Tro-$Ac_5$c-$Ac_5$c-$Ac_5$c-$Ac_5$c) (**2**) shows very similar torsion angles and conformational properties for the $\alpha$,$\alpha$-disubstituted $\alpha$-amino acids Aib and $Ac_5$c. The results of the conformational analysis of **1** in $CDCl_3$ solution by

NMR spectroscopy, followed by MD simulations, indicate that the average structure in solution at room temperature is almost the same as that in the solid state.

## Experimental Part

1. *X-Ray Crystal-Structure Determination of* **1** (see *Table 5*, and *Figs. 1* and *2*)[3]). All measurements were made on a *Rigaku AFC5R* diffractometer with graphite-monochromated Mo$K_\alpha$ radiation ($\lambda = 0.71069$ Å) and a 12-kW rotating anode generator. The $\omega/2\theta$ scan mode was employed for data collection. The intensities were corrected for *Lorentz* and polarization effects, but not for absorption. Data collection and refinement parameters are given in *Table 5*. A view of the molecule and a packing diagram are shown in *Fig. 1* and *Fig. 2*, resp. The structure was solved by direct methods using *SHELXS86* [20], which revealed the positions of all non-H-atoms. There are two independent molecules in the asymmetric unit, but the conformations of the molecules are significantly different, so that additional crystallographic symmetry is not possible. The non-H-atoms were refined anisotropically. All of the amide H-atoms were placed in the positions indicated by a difference electron-density map, and their positions were allowed to refine together with individual isotropic displacement parameters. All remaining H-atoms were fixed in geometrically calculated positions ($d$(C–H) = 0.95 Å), and they were assigned fixed isotropic displacement parameters with a value equal to 1.2 $U_{eq}$ of the parent C-atom.

Table 5. *Crystallographic Data of Compound* **1**

| | |
|---|---|
| Crystallized from | MeOH/AcOEt/$CH_2Cl_2$ |
| Empirical formula | $C_{25}H_{36}N_4O_6$ |
| Formula weight [g · mol$^{-1}$] | 488.58 |
| Crystal color, habit | colorless, prism |
| Crystal dimensions [mm] | 0.30 × 0.30 × 0.43 |
| Temp. [K] | 173(1) |
| Crystal system | monoclinic |
| Space group | $P2_1/n$ |
| $Z$ | 8 |
| Reflections for cell determination | 25 |
| $2\theta$ Range for cell determination [°] | 23 – 36 |
| Unit-cell parameters $a$ [Å] | 17.052(6) |
| $b$ [Å] | 16.687(5) |
| $c$ [Å] | 18.607(3) |
| $\beta$ [°] | 90.30(2) |
| $V$ [Å$^3$] | 5294(2) |
| $D_x$ [g cm$^{-3}$] | 1.226 |
| $\mu$(Mo$K_\alpha$) [mm$^{-1}$] | 0.0881 |
| $2\theta_{(max)}$ [°] | 55 |
| Total reflections measured | 12995 |
| Symmetry-independent reflections | 12154 |
| Reflections used [$I > 2\sigma(I)$] | 7513 |
| Parameters refined | 663 |
| Final $R$ | 0.0519 |
| $wR$ ($w = [\sigma(F_o) + (0.005\ F_o)^2]^{-1}$) | 0.0451 |
| Goodness-of-fit | 1.752 |
| Final $\Delta_{max}/\sigma$ | 0.0003 |
| $\Delta\rho$(max; min) [e Å$^{-3}$] | 0.38; –0.25 |

[3]) Crystallographic data (excluding structure factors) for structure **1** reported here have been deposited with the *Cambridge Crystallographic Data Centre* as supplementary publication No. CCDC-145105. Copies of the data can be obtained, free of charge, on application to the CCDC, 12 Union Road, Cambridge CB2 1EZ, UK (fax: +44-(0)1223-336033; e-mail: deposit@ccdc.cam.ac.uk).

Refinement of the structure was carried out on *F* by full-matrix least-squares procedures, which minimized the function $\Sigma w(|F_o|-|F_c|)^2$.

Neutral-atom-scattering factors for non-H-atoms were taken from [21a], and scattering factors for H-atoms were taken from [22]. Anomalous dispersion effects were included in $F_{calc}$ [23]; the values for $f'$ and $f''$ were those of [21b]. All calculations were performed with the *TEXSAN* crystallographic software package [24].

2. *NMR Measurements of (*R*)-***1***.* The ROESY spectrum was measured at 275 K on a *Bruker DRX-600* spectrometer by the phase-sensitive, *States-TPPI* method, 2D ROESY [25] experiment with cw spinlock for mixing. A data matrix of $512 \times 2048$ complex points in $t_1$ and $t_2$, resp., were recorded. In both dimensions, data were weighted with a shifted sine-bell function and the $t_1$ data newly zero-filled to 1024 complex points prior to the *Fourier* transformation.

3. *Molecular-Dynamics Simulations of (*R*)-***1***.* Starting structures were taken from the final set of NMR structures of (*R*)-**1**. All calculations were performed with the *GROMOS96* program package in conjuction with the *GROMOS96* 43A1 force field [26]. The unusual amino acid residues Aib and Tro were created based on the similar residues Ala and Phe, respectively, with the default force field parameters and atom types.

Starting from the minimized structures, molecular-dynamics (MD) simulations were performed *in vacuo* and in solution. In case of the simulations in solution, the molecule was surrounded by $CHCl_3$ molecules [27] in a rectangular box (with minimum distances from the molecule to the box wall of 14 Å) under periodic boundary conditions. The MD simulations were performed by an isothermal-isobaric simulation algorithm. The temp. and the pressure were maintained (300 K and 1 atm, resp.) by weak coupling to an external temp. bath with a coupling constant of 0.1 and 0.5 ps, resp. A cut-off for the non-bonded interactions of 1.4 nm was chosen. After an equilibration period of 21 ps, the simulations were performed over a time scale of 2 ns (up to 6 ns).

## REFERENCES


[1] E. Benedetti, *Biopolymers* **1996**, *40*, 3.
[2] C. Toniolo, M. Crisma, F. Formaggio, G. Valle, G. Cavicchioni, G. Precigoux, A. Aubry, J. Kamphuis, *Biopolymers* **1993**, *33*, 1061.
[3] I. L. Karle, P. Balaram, *Biochemistry* **1990**, *29*, 6747.
[4] B. V. Venkataram Prasad, P. Balaram, *Crit. Rev. Biochem.* **1984**, *16*, 307.
[5] C. Toniolo, E. Benedetti, *TIBS* **1991**, *16*, 350.
[6] J. L. Flippen, I. L. Karle, *Biopolymers* **1976**, *15*, 1081.
[7] G. Zanotti, M. Saviano, G. Saviano, T. Tancredi, F. Rossi, C. Pedone, E. Benedetti, *J. Pept. Res.* **1998**, *51*, 460.
[8] E. Escudero, X. Vidal, X. Solans, E. Peggion, J. A. Subirana, *J. Pept. Sci*. **1996**, *2*, 59.
[9] B. Di Blasio, F. Rossi, E. Benedetti, V. Pavone, M. Saviano, C. Pedone, G. Zanotti, T. Tancredi, *J. Am. Chem. Soc*. **1992**, *114*, 8277.
[10] F. Rossi, M. Saviano, P. Di Talia, B. Di Blasio, C. Pedone, G. Zanotti, M. Mosca, G. Saviano, T. Tancredi, K. Ziegler, E. Benedetti, *Biopolymers* **1996**, *40*, 465.
[11] I. Dannecker-Dörig, Ph.D. thesis, Universität Zürich, 1995.
[12] F. S. Arnhold, Ph.D. thesis, Universität Zürich, 1997.
[13] K. N. Koch, A. Linden, H. Heimgartner, *Helv. Chim. Acta* **2000**, *83*, 233.
[14] C. K. Johnson, '*ORTEPII*, Report ORNL-5138', Oak Ridge National Laboratory, Oak Ridge, Tennessee, 1976.
[15] T. Ashida, Y. Tsunogae, I. Tanaka, T. Yamane, *Acta Crystallogr.*, *Sect. B* **1987**, *43*, 212.
[16] R. Taylor, O. Kennard, W. Versichel, *Acta Crystallogr., Sect. B* **1984**, *40*, 280.
[17] S. Vijayalakshmi, R. Balaji Rao, I. L. Karle, P. Balaram, *Biopolymers* **2000**, *53*, 84.
[18] H. King, A. D. Palmer, *J. Chem. Soc*. **1922**, *121*, 2577.
[19] P. Güntert, C. Mumenthaler, T. Herrmann, *J. Mol. Biol*. **1997**, *273*, 283.
[20] G. M. Sheldrick, '*SHELXS86*', *Acta Crystallogr., Sect. A* **1990**, *46*, 467.
[21] a) E. N. Maslen, A. G. Fox, M. A. O'Keefe, in 'International Tables for Crystallography', Ed. A. J. C. Wilson, Kluwer Academic Publishers, Dordrecht, 1992, Vol. C, Table 6.1.1.1, pp. 477–486; b) D. C. Creagh, W. J. McAuley, *ibid*. Table 4.2.6.8, pp. 219–222.
[22] R. F. Stewart, E. R. Davidson, W. T. Simpson, *J. Chem. Phys.* **1965**, *42*, 3175.
[23] J. A. Ibers, W. C. Hamilton, *Acta Crystallogr*. **1964**, *17*, 781.

[24] '*TEXSAN:* Single Crystal Structure Analysis Software', Version 5.0, Molecuar Structure Corporation, The Woodlands, Texas, 1989.
[25] A. Bax, D. G. Davis, *J. Magn. Reson*. **1985**, *63*, 207.
[26] W. F. van Gunsteren, S. R. Billeter, A. A. Eising, P. H. Hünenberger, P. Krüger, E. A. Mark, W. R. P. Scott, I. G. Tironi, in 'Biomolecular Simulation, The GROMOS96 Manual and User Guide', Vdf Hochschulverlag AG an der ETH-Zürich, Zürich, 1996.
[27] I. G. Tironi, W. F. van Gunsteren, *Mol. Phys.* **1994**, *83*, 381.

*Received November 10, 2000*